ELSEVIER

Lithos 50 (2000) 305–324

LITHOS

www.elsevier.nl/locate/lithos

The Ordovician chondrite from Brunflo, central Sweden III. Geochemistry of terrestrial alteration

Beda A. Hofmann [a,*], Jan Olov Nyström [b], Urs Krähenbühl [c]

[a] *Naturhistorisches Museum Bern, Bernastrasse 15, CH-3005 Bern, Switzerland*
[b] *Swedish Museum of Natural History, S-10405 Stockholm, Sweden*
[c] *Departement für Chemie und Biochemie, Universität Bern, Freiestrasse 1, CH-3012 Bern, Switzerland*

Received 26 January 1999; accepted 26 August 1999

Abstract

The fossil H chondrite Brunflo, found in a slab of Ordovician limestone from central Sweden, is pervasively altered to an assemblage dominated by calcite and barite. The meteorite is surrounded by a 15–20 cm wide zone of lighter colors than the unaffected limestone due to dissolution of hematite. Here we present detailed geochemical analyses of two meteorite samples, 14 limestone samples at distances from 0 to 29 cm along two profiles from the meteorite, and a reference sample of Brunflo limestone. Element concentrations in Brunflo and surrounding bleached limestone have been strongly disturbed during two stages of alteration (early oxygenated and deep burial). In the meteorite, the Ni/Co ratio has changed from an initial value of 20 to 0.8 and redox sensitive elements like V, As, Mo, Re and U are strongly enriched. The sulfur isotope composition of barite from Brunflo ($\delta^{34}S = +35‰$) indicates initial loss of meteoritic sulfide, followed by later accumulation of sea water sulfate as barite. During deep burial under more reducing conditions, reduction processes supported by an externally derived reductant possibly derived from alum shale underlying the limestone, were largely responsible for the observed redox phenomena. In spite of massive redistribution of many elements, concentrations of Pt, Ir and Au remain at chondritic levels. The geochemistry and mineralogy of alteration determined for Brunflo are similar to those in ''reduction spots'' in red beds, where accumulation of a similar suite of elements (except Mo, Re) occurred as a result of isolated reduction activity.

Keywords: Meteorite; Ordovician; Geochemistry; Redox; Element mobility

1. Introduction

The stony meteorite Brunflo is one of the very few fossil meteorites known (Thorslund and Wickman, 1981; Thorslund et al., 1984). Brunflo was found in a Middle Ordovician red limestone deposited under oxidizing conditions at a low sedimentation rate. Seventeen fossil meteorites have been discovered during the last years at Österplana, Kinnekulle, in southern Sweden (58°35′N 13°26′E), also in red (and gray) limestone of Middle Ordovician age but about 5 Ma older than the limestone hosting Brunflo (Nyström et al., 1988; Schmitz et al., 1996, 1997).

A conspicuous feature of Brunflo is a 15–20 cm wide multicolored zonation around the 7×8 cm

* Corresponding author. Fax: +41-31-350-74-99; e-mail: beda.hofmann@nmbe.unibe.ch

0024-4937/00/$ - see front matter
PII: S0024-4937(99)00061-4

cross section of the meteorite exposed on a polished rock slab. Nyström and Wickman (1991) studied the secondary mineralogy of Brunflo and reported a range of minerals unknown to unaltered meteorites including Co–Ni–arsenides and V-bearing illite. Both the zonation around Brunflo and its secondary mineralogy show a strong similarity to so-called reduction spots in red bed sediments. Reduction spots are the result of small-scale diffusive redox systems in red bed sediments with uncertain cause of the reductive processes and are enriched in many elements, including Co, Ni, As and V (Hofmann, 1990, 1991, 1992a). A detailed geochemical investigation of the terrestrial alteration in and around the Brunflo meteorite was thus undertaken in order to characterize element remobilizations in a redox gradient established between a chondrite and oxidized carbonate-rich sediment. Studies of element mobility in redox gradients are relevant to the safety assessment of radioactive waste disposal (Miller et al., 1994; Hofmann, 1999). Also, knowledge of geochemical changes induced by meteorites in sediments will facilitate their recognition in cases where no indicator mineral such as chromite is left.

2. Regional geology

The fossil chondrite was found in the Rödbrottet limestone quarry near Brunflo, close to the geographic center of Sweden (63°5′N 14°53′E; Thorslund et al., 1984). Brunflo fell into a shelf sea at a water depth probably exceeding 200 m (Lindström et al., 1996). The Ordovician platform limestone which hosts the meteorite was deposited under calm conditions with sedimentation rates of 0.2–0.3 cm/1000 years (Jaanusson, 1976, 1982). The limestone is about 50 m thick at Brunflo and is underlain by Cambrian alum shale with a typical thickness of 20 m and the Precambrian basement (Lindström et al., 1996). The alum shale is of particular interest for this study due to its elevated contents of V, U, Mo, Ni and many other rare elements (Leventhal, 1991).

The Lower Paleozoic sequence at Brunflo belongs to the lower allochthon of the Jämtland Caledonides (Bergström and Gee, 1985; Bruton et al., 1985). The tectonic movement of the alum shale and limestone in the area was probably of the order of 3 km (Lindström et al., 1996). Brunflo is located close to the eastern boundary of the partly eroded Caledonian nappe cover. Since the original nappe cover extended farther east, the maximum burial depth of the meteorite is uncertain. The color alteration of conodonts in the hosting limestone suggests that the meteorite experienced temperatures of 200 to 300°C, probably due to burial beneath Caledonian nappes (Löfgren, 1978; Bergström, 1980). Kisch (1980) reported values in the diagenetic range for the Brunflo limestone in a regional study of illite crystallinity and vitrinite reflectivity.

Several impact structures of Ordovician age are known from the region (Lindström and Sturkell, 1992; Puura and Suuroja, 1992; Therriault and Lindström, 1995) which, probably, are unrelated to the fossil meteorites.

3. Previous studies of Brunflo

Previous studies of Brunflo include a first report (Thorslund and Wickman, 1981), a general description focusing on its primary structure and minerals (Thorslund et al., 1984) and a description of its secondary mineralogy (Nyström and Wickman, 1991). Based on the proportion of different chondrule types and the composition of chromite (the only primary mineral preserved with the exception of rare chrome spinel), Thorslund et al. (1984) concluded that Brunflo most probably is a H4–H5 chondrite. Considering the small differences and overlaps in composition between chromites in H3–H6 chondrites (Bunch et al., 1967), Brunflo is treated as an unspecified H-group chondrite in the present paper.

The chondritic structure of Brunflo is locally very well-preserved, in spite of the pervasive alteration. The original minerals are almost totally replaced by calcite, barite, a Cr–V-bearing illite-type layer silicate and small or trace amounts of many other secondary minerals described by Nyström and Wickman (1991). They are summarized in Table 1 together with a few newly identified phases. There are several Ni–Co phases, the most common being close to $NiCoAs_2S_2$ in composition, indicating a decrease of the overall Ni/Co ratio from 20 to 1 during alteration. The secondary mineralogy is highly vari-

Table 1
Primary and secondary mineralogy of the Brunflo chondrite

Major primary minerals (based on H chondrites, mode from McSween et al., 1991)	
	mode
Olivine $(Mg,Fe)SiO_4$	35.0
Orthopyroxene $(Mg,Fe)SiO_3$	26.2
Kamacite $Fe_{0.95}Ni_{0.05}$	
Taenite $Fe_{0.8}Ni_{0.2}$	Total metal 18.0
Plagioclase	9.0
Troilite FeS	5.5
Clinopyroxene $(Ca,Mg,Fe)SiO_3$	4.1
Chromite $(Fe,Mg)(Cr,Al,Ti,V)_2O_4$	0.76
Cr-spinel $(Fe,Mg)(Al,Cr)_2O_4$	tr.
Graphite or poorly graphitized carbon C (this work)	tr.
Secondary minerals (from Nyström and Wickman, 1991)	
	mode
Calcite $CaCO_3$	67
Barite $BaSO_4$	17
V–Cr-rich illite	10
Cobaltite–gersdorffite (CoNi)AsS	3
Quartz SiO_2	2
Chromite $(Fe,Mg,Zn)(Cr,Al)_2O_4$	0.4
Chalcopyrite $CuFeS_2$	0.3
Titanium dioxide TiO_2	0.2
Molybdenite MoS_2 (this work, mode based on Mo content)	0.2
''Bornite'' Cu_5FeS_4	
''Chalcocite'' $Cu_{1.66}S$	
Galena PbS	
Gersdorffite NiAsS	
Hematite Fe_2O_3 (at boundary to limestone, this work)	
Native nickel Ni	
Nickeline NiAs	
Orcelite CoAs	
Pyrite FeS_2	
Rammelsbergite $NiAs_2$	
Safflorite $CoAs_2$	
Sphalerite ZnS	
U-bearing titanium dioxide $(Ti,U)O_2$ (this work)	

able over small distances, demonstrating nonequilibrium conditions during formation. The major chondritic constituents Mg and Fe are almost completely lost and Si is strongly depleted, while Ca, Ba, carbonate, As, S, K, P, Co, Sr, V, Cu and F accumulated during the alteration. Nyström and Wickman (1991) suggested that most alteration reactions took place in a calcareous mud-sea water system before the mud was lithified to limestone, but regional heating during Caledonian nappe overthrusting and during an impact event 20–40 Ma after the fall of Brunflo (Lindström and Sturkell, 1992; Lindström et al., 1996) might also have played a role.

Thorslund et al. (1984) described four alteration zones around the meteorite: zone 1 (0–30 mm from the stone, greenish gray), zone 2 (30–80 mm from the stone, grayish red-brown), zone 3 (80–130 mm from the stone, yellowish red-brown) and zone 4 (beyond 130 mm, slightly darker red-brown than the normal limestone at the stratigraphic level of the Brunflo chondrite). The transitions between the different zones are gradual over several millimeters to a couple of centimeters.

4. Samples, methods, and data selection

4.1. Samples

The following sampling approach was used to obtain maximum information from the small amount

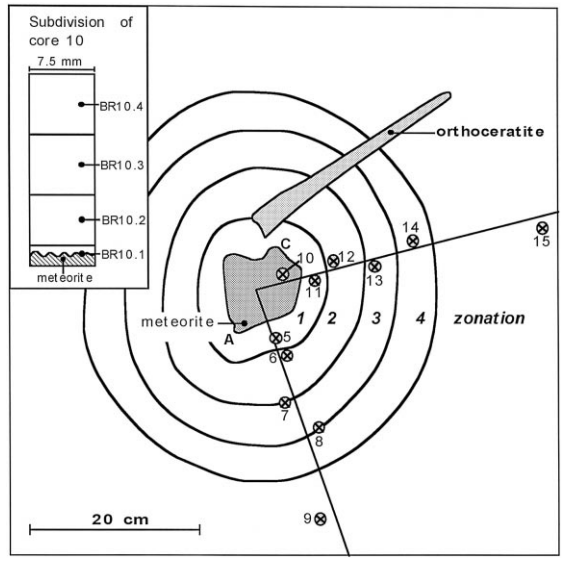

Fig. 1. Sketch of the rock slab containing the Brunflo chondrite with projected positions of the drill cores obtained from the back of the slab. The two cores from the meteorite are not shown. The inset illustrates the subdivision of core BR10 that contains the meteorite–limestone contact. A and C: meteorite corners as labelled in Fig. 2 of Thorslund et al. (1984), given for orientation.

of material available for investigation. The meteorite and surrounding limestone was sampled with a drilling machine from the back of the slab by one of us (J.O.N.) in 1979. The positions of the cores (4–20 mm long; diameter 7.5 mm) are illustrated in Fig. 1. Eleven cores were drilled in the limestone, distributed along two profiles toward the meteorite, and two short cores come from the meteorite itself. Eight polished thin sections of the meteorite were also studied. The limestone cores were split along their length and one half of each sample was used for analysis and the second half was preserved. A limestone core penetrating the outermost millimeter of the meteorite (BR10) was divided into four parts (Fig. 1). In total, two meteorite samples and 14 samples of enclosing limestone from the slab were analyzed. In order to evaluate the relevance of the analytical results for such small samples from a visually heterogeneous rock, a reference sample of limestone (BR1) weighing about 1 kg was analyzed employing various methods. This sample was collected by Lars Karis (Geological Survey of Sweden) from the Rödbrottet quarry (Swedish National Grid reference 699805/145308, Economic Map sheet 18F 9a Brunflo, scale 1:10 000). It was situated 1.2 to 1.3 m below the Lower/Middle Ordovician boundary in the Holen topoformation, i.e., from the same stratigraphic level as the limestone hosting Brunflo. All core samples selected for analysis were hand ground in an agate mortar; BR1 was crushed in a jaw crusher and ground in an agate mill under alcohol. A description of the samples used in this study is given in Table 2.

4.2. Analytical methods

The 16 core samples were analyzed with ICP-MS, ICP-OES and colorimetric methods after dissolution in a mixture of $HCl/HNO_3/HF$ in teflon containers. The ICP-MS analyses were carried out at Trace Analytic SA (Morges, Switzerland), the ICP-OES analyses at LambdaMax laboratories (Bern, Switzer-

Table 2
Sample description

No.	Weight (g)	Distance to meteorite (mm)	Color (rock color chart[a])		Description	Bulk radioactivity (counts/min[b])
BR3b	0.82	0	olive black	5Y 2/1	meteorite	3.4
BR4	0.17	0	olive black	5Y 2/1	meteorite	1.8
BR10.1	0.06	1	dark green	5GY4/1	meteorite–limestone	26.0[c]
BR10.2	0.59	4	gray	N6	limestone	26.0[c]
BR10.3	0.70	8	gray	N6	limestone	< 0.5[c]
BR10.4	0.70	14	gray	N6	limestone	< 0.5[c]
BR5	0.54	20	gray	N6	limestome	1.7
BR11	0.55	20	gray	5YR5/1	limestone	< 0.5
BR12	0.50	40	gray	5YR5/1	limestone	0.8
BR6	0.49	48	gray-red	5YR5/1	limestone	< 0.5
BR13	0.59	87	red	5R4/2	limestone	0.9
BR7	0.58	95	gray-red	5YR5/1	limestone	< 0.5
BR8	0.94	135	red	5R4/2	limestone	1.1
BR14	0.45	139	red	5R4/2	limestone	< 0.5
BR9	0.73	238	red	5R4/2	limestone	< 0.5
BR15	0.47	290	red	5R4/2	limestone	2.0
BR1	ca. 1 kg	–	red	5R4/2	limestone reference sample	< 0.5

[a] Rock color chart distributed by the Geological Society of America.
[b] Background (21.9 counts/min) subtracted, 20 min counting time. Relative values are significant only.
[c] Samples BR10.1/2 and BR10.3/4 were measured combined before splitting.

land) and the colorimetric analyses at the Mineralogisch-petrographisches Institut, Bern University. Twelve of the samples were also analyzed with INAA at Interfacultair Research Instituut of Delft Technical University (Delft, The Netherlands) and four at the University of Bern by one of us (UK). Additional analyses were made of reference sample BR1 with XRF (Mineralogisch-petrographisches Institut, Bern University), INAA, ICP-OES, FA-DCP (Fire-Assay preconcentration-Direct Current Plasma-OES, Bondar Clegg, Toronto) and ICP-OES (Centre de Recherches Pétrographiques et Géochimiques, Vandoeuvre, France).

Microprobe analyses of Cr, V, Ni and Co in the meteorite–limestone transition zone were made with a Cameca SX-50 microprobe at Bern University, operated at 15 kV with a beam current of 20 nA and in scanning mode, each analysis covering an area of 30 by 55 μm. Counting times were 30 s on peaks and 15 s on backgrounds.

Alpha particle autoradiographs were prepared using Kodak LR II film with an exposure time of up to 5 months, followed by etching in 2.5 N KOH at 60°C. Gamma-Spectroscopy was performed using HPGE detectors and a Nuclear Data MCA system for data collection and processing.

Sulfur isotope ratios for barite were determined in the laboratory of Prof. J. Hoefs, Göttingen University, using a standard gas mass spectrometry method. The mineralogy of BR1 was determined with XRD on whole rock powder and decarbonated samples using LiF as internal standard.

4.3. Data selection

Data for each core sample are based on a single analysis with ICP-MS, INAA, and colorimetry (for Fe), the host rock samples were additionally analyzed with ICP-OES. In order to obtain a consistent set of concentration data for the individual elements, consistent results (within error limits) for different analytical methods were averaged. In uncertain cases, the results for the most consistent method(s), based on multiple analyses of BR1, were chosen. The consistency of the analytical methods was evaluated by comparison with results from other methods for BR1.

5. Results

5.1. Radioactivity

Prior to other treatment, the bulk radioactivity of the samples was measured with a Geiger–Müller tube sensitive to α,β and γ radiation to detect anomalous samples. The background-corrected values, which can only be used qualitatively, are given in Table 2. These determinations revealed that the meteorite samples, and especially sample BR10.1 that contains the meteorite–limestone contact, are significantly more radioactive than the limestone. Gamma-Spectroscopy showed that these samples are enriched in U but not in Th or K.

Table 3
Miscellaneous data for Brunflo and host rock reference sample BR1

	Unit	
Geometry		
Area of meteorite in section, estimated	cm^2	60.50
Radius of meteorite, estimated	cm	4.4
Volume of meteorite, calculated from radius	cm^3	357
Density and weight		
Host rock bulk density (BR1), $n = 4$, $s = 0.008$	g/cm^3	2.73
Meteorite bulk density (BR 3b)	g/cm^3	3.41
Meteorite grain density, calculated from mode	g/cm^3	3.16
Model weight of meteorite (calculated from volume and calculated density)	g	1128
Sulfur isotopic composition of barite		
BR3b	$\delta^{34}S$	+34.68
BR3b	$\delta^{34}S$	+35.73
Mineralogy of sample BR1		
Based on gravimetric determination of HCl-insoluble residue, XRD of whole rock and HCl-insoluble residue		
Calcite	wt.%	83.3
Quartz	wt.%	4.5
Hematite (based on Fe depletion near meteorite)	wt.%	0.6
Clay minerals (by difference, illite:chlorite ~ 4:1)	wt.%	11.6
Illite ''crystallinity'' (Kuebler width)	$\Delta°2\Theta$	0.45

Table 4
Analytical data for host rock reference sample BR1
Values in italics were excluded from calculation of average.
Lab codes: BC = Bondar Clegg, CRPG = Centre de Recherches Pétrographiques et Géochimiques, LMAX = Lambda Max, TA = Trace Analytic SA, IRI = Interfacultair Reactor Instituut, UNIBE = University of Bern.
METHOD CODES: ICP-OES: Inductively Coupled Plasma Optical Emission Spectroscopy, ICP-MS: Inductively Coupled Plasma-Mass Spectroscopy, INAA: Instrumental Neutron Activation, FA-DCP: Fire Assay-Direct Current Plasma optical emission spectroscopy, XRF: X-ray Fluorescence, COLO: Colorimetry, GFAA: Graphite Furnace Atomic Absorption spectroscopy, GRAV: gravimetric determination of HCl residue.

Method		ICP-CES (FA-DCP)	ICP-OES	ICP-OES	ICP-MS	ICP-MS	INAA	INAA	INAA	XRF	Others	Source	Average used[a]
Laboratory		BC	CRPG	LMAX	TA	TA	BC	IRI	UNIBE	UNIBE			
El	unit												
Li	ppm	14				7							11
Be	ppm		0.5			0.2							0.33
B	ppm					38							38
Na	%	*0.25*	0.02				0.02	0.02	0.02	*0.10*			0.02
Mg	%	0.36	0.42	0.35		0.36				*0.55*			0.37
Al	%	1.41	1.62	1.53						1.53			1.52
Si	%		4.43							4.44			4.44
P	%		0.02	< 0.02						0.02			0.02
K	%	0.83	0.52	0.68				0.74	0.74	0.66			0.69
Ca	%	> 10	33.46	*28.60*				35.10		*31*	33.4 GRAV		34.0
Sc	ppm	3	*14.8*		*2.2*		5.7	5.0	4.9				4.7
Ti	%	0.08	0.09		0.075	0.067				0.10			0.08
V	ppm	18	23	21	< 0.2	17				22			20
Cr	ppm	31	30	21	*18*	*13*	25	21	21	27			25
Mn	ppm	2380	2090	2400	2173	*690*				2090			2230
Fe	%	1.30	1.27	1.32		*1.10*	*1.5*	1.28	1.46	*1.80*	1.35 COLO	UNIBE	1.33
Co	ppm	< 1	9.0		7.5	6.9		4.8	6.3				6.9
Ni	ppm	23	34		31	29	*13*	< 33		*46*			29
Cu	ppm	6	7		4.6	6				*17*			5.8
Zn	ppm	16	9		13	10		< 33		*37*			12
Ga	ppm	*90*	*10*		3.6	5				*1*			4.1
Ge	ppm				0.7	2							1.4
As	ppm	*7*			< 0.2	*0.02*	*2.4*	0.70	0.70	< 2			0.7
Br	ppm					*12*	2	2					2.0
Rb	ppm		28		36	34	31	32		26			31
Sr	ppm	191	207		199	206		*303*		181			197
Y	ppm	*9*	12.3		*2*	*9*				*9*			12
Zr	ppm	36	32		21	25		*66*		28			28
Nb	ppm	*31*	< 5		2.1	2.3				*1*			2.2
Mo	ppm	< 1			0.4		< 1						0.4
Ag	ppm	< 0.2			0.7	0.7							0.7
Cd	ppm	*2.2*			0.06	0.02	< 5						0.04

Sn	ppm	< 5			0.05	0.2						0.3
Sb	ppm				0.6	0.4	1	0.9				0.7
Cs	ppm				*5.2*	2.5	2	1.8				2.1
Ba	ppm	82	77	63	90	113	96	98	*54*			88
La	ppm	*7*	10.4		*4.6*	*8.2*	*14*	11.0				11
Ce	ppm		23.6		*10*	*19.0*	*30*	23.6				24
Pr	ppm				1.5	2.5						2.0
Nd	ppm		10.5		*7.7*	*14.0*		16.0				13.3
Sm	ppm		2.5		*1.9*	*3.1*	2.3	2.2				2.3
Eu	ppm		0.55		*0.4*	*0.7*	< 1	0.5				0.5
Gd	ppm		2.3		*1.8*	*3.7*						2.3
Tb	ppm				0.3	0.6	< 5	0.3				0.4
Dy	ppm		1.89		*1.6*	*2.5*						1.9
Ho	ppm				*0.2*	0.4						0.4
Er	ppm		1.11		*0.8*	*1.6*						1.1
Tm	ppm				*0.2*	0.3						0.3
Yb	ppm		0.8		*0.7*	*1.3*	< 2	1.0				0.9
Lu	ppm		0.12		< 0.2	*0.1*	0.2	0.2				0.2
Hf	ppm				1.3	1.2	1	1.0				1.1
Ta	ppm	*8*			0.3	0.2	< 0.5	0.2				0.2
W	ppm				1.2	1.0	< 1	0.8				1.0
Au	ppb	(3)					2	< 7.5				2.5
Tl	ppm	< 0.1			*0.25*	0.04						0.04
Pb	ppm	*31*			3.3	1.9			3.1	2.2 GFAA	UNIBE	2.6
Bi	ppm	< 5			< .2	0.02						0.02
Th	ppm		*32*		*0.73*	*5.9*	2.7	2.6	< 1			2.63
U	ppm				0.5	0.6	0.4	0.3	*1.5*			0.44

[a]Referred to as ‘‘best values’’.

5.2. Mineralogy and geochemistry of host rock reference sample BR1

Bulk mineralogy and clay mineral data for sample BR1 are presented in Table 3. The Brunflo host rock is an impure clayey limestone containing 83% calcite, the rest consisting mostly of clay minerals and quartz. The clay mineral fraction is composed of the two phases illite and chlorite (approximately 80% illite and 20% chlorite). Illite ''crystallinity'' measured by repeated scanning of the (001) peak and compared with the NAU12 standard yielded a half-width of 0.45 $\Delta°2\Theta$ CuKα (Kisch, 1991). This value indicates conditions close to the transition between diagenesis and onset of low-grade metamorphism, consistent with the results of Kisch (1980) who reported low crystallinity values (> 0.5) for the Brunflo area.

Major and trace element data for sample BR1 obtained from different methods and laboratories are presented in Table 4. The average of the up to nine independent consistent analyses are also given. These values serve as a background concentration (here referred to as ''Best values'') to which the analytical data for the limestone core samples can be compared.

5.3. Mineralogy of the meteorite–limestone contact zone

The mineralogical investigations reported here were concentrated to the contact zone between the meteorite and the surrounding limestone, since Nyström and Wickman (1991) described the mineralogy of the meteorite in detail. Inspection in reflected light of a polished chip (4.5 by 5.5 mm) from the radioactive core sample BR10.1 (Fig. 1) shows that the 0.5–1 mm thick end part corresponding to the contact is composed of coarsely crystalline calcite, barite, chromite grains, finely dispersed hematite and a Ti dioxide phase, probably anatase (Fig. 2). The composition is similar to that of the altered bulk meteorite. The original fusion crust cannot be identified due to the pervasive alteration.

Other secondary minerals in the near-contact zone include Cr-V-bearing illite and a very fine-grained (< 1 to 3 μm) uraniferous titanium dioxide. The distribution of alpha-emitters (mostly uranium) across the meteorite-limestone contact is illustrated in Fig. 3. Microprobe analyses of the Ti dioxide show an average atomic U/Ti-ratio of 0.18, much lower than the ratio in brannerite (0.5). Although microprobe totals are low due to the small size of the analyzed

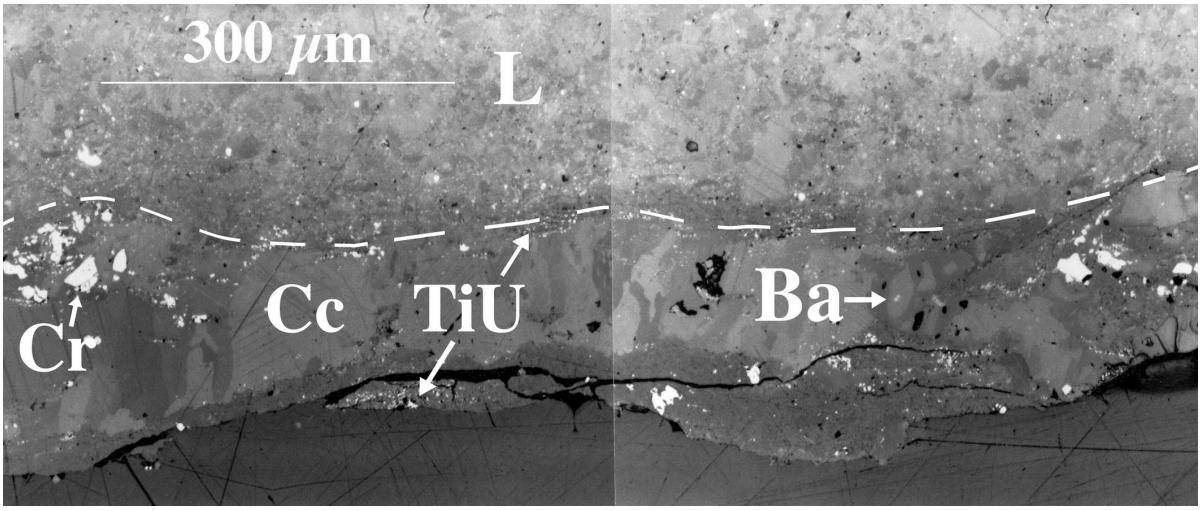

Fig. 2. Photomicrograph of the meteorite–limestone transition zone. Cr = chromite, Cc = calcite, TiU = uraniferous titanium dioxide, Ba = barite, L = limestone. The broken line outlines the approximate boundary between the meteorite and the enclosing limestone.

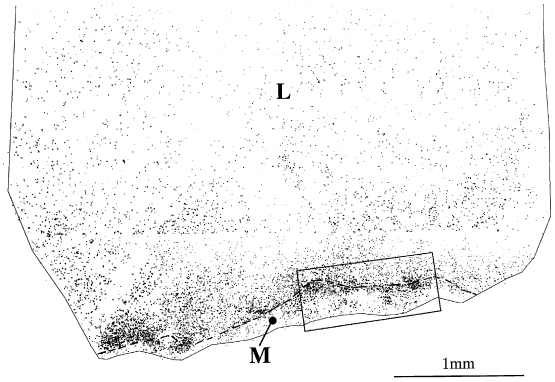

Fig. 3. Alpha-autoradiograph (5 months exposure) of the meteorite–limestone transition zone showing a significant enrichment of alpha-emitters (uranium) close to the meteorite–limestone boundary. The area shown in Fig. 2 is marked with a frame (M = meteorite, L = limestone).

grains, the covariation of U, Ti and Pb demonstrates that U and Pb are bound to the Ti dioxide phase. The Pb is probably radiogenic; the microprobe results yield an average Pb/U-ratio of 0.074 ± 0.017, corresponding to a chemical ''age'' of 434 ± 100 Ma, which is consistent with the terrestrial age of the meteorite (460–470 Ma; Nyström and Wickman, 1991).

5.4. Mineralogy of the fossil meteorite

The mineralogical results of Nyström and Wickman (1991) are summarized in Table 1. The following additional results were obtained during this study.

5.4.1. U-bearing phase

Alpha-autoradiographs and chemical analyses show a significant enrichment of diffusely distributed U in the interior of the meteorite. Uranium was detected by microprobe analysis in amounts of up to 0.79 wt.% (average 0.25%, $n = 16$) in dark brown Ti dioxide grains up to 50 μm in size. The more common light brown or yellow Ti dioxide grains do not contain detectable U. An average Pb/U ratio of 0.28 for this phase indicates the presence of significant amounts of nonradiogenic Pb, U loss or both.

5.4.2. Mo-phase

Molybdenite or a similar Mo-rich sulfide was identified as numerous tiny aggregates with grain sizes of < 1 to a few μm, partly surrounding Co–Ni–sulfarsenides.

5.4.3. Graphite

In one polished thin section (4A) a spheroidal aggregate of graphite or poorly graphitized carbon 25 μm in diameter was found. This graphite may be a primary meteoritic relict mineral.

5.5. Geochemistry of the Brunflo chondrite

The bulk density of the Brunflo meteorite as determined for one sample and grain density calculated from the mode yielded values (3.41, 3.16 g/cm^3, Table 3) close to the range of H chondrites (3.4–3.9 g/cm^3, Mason, 1971). Furthermore, the well-preserved chondrite structure argues against a strong volume change during the alteration. Concentrations in the altered meteorite can therefore be compared directly with chondritic values, within the limits of uncertainty.

The combination of modal abundance and mineral compositions given by Nyström and Wickman (1991) for Brunflo allows the calculation of its bulk chemical composition with regard to major and some minor elements. This calculated composition is given in Table 5 where it is compared with the analyses of the two drill cores from the meteorite. The agreement between calculated composition and analytical values is quite good, considering the small size of the analyzed samples and the heterogeneity of the secondary mineralogy. The low Ni/Co ratio (0.96) obtained from microprobe analysis and mode was confirmed by bulk analysis (0.82). In contrast, a typical chondritic Ni/Co ratio would be 20. Fig. 4 shows the average composition of the Brunflo chondrite together with host rock sample BR1 normalized to average H chondrites (Mason, 1971). Element enrichments are highest for Ba (85 000), Bi (16 000), As (6800), Tl (3800), U (2500) and Mo (1200). While Ba, As, U and Mo are present as main or minor constituents of mineral phases, no hosts containing Bi or Tl could be identified.

The concentrations of C, Al, Si, S and Mn in Brunflo were not determined during this study but their behavior can be deduced from concentrations calculated from the mode. Ratios of Brunflo/average H chondrite (Mason, 1971) are (wt.%): C =

Table 5
Analytical data for Brunflo and its host rock
1: ICP-MS; 2: INAA; 3: ICP-OES; 4: ICP-OES/ICP-MS averaged; 5: ICP-MS/INAA averaged; 6: colorimetry/ICP-OES/INAA averaged; 7: ICP-IV BR1 concentrations in italics are upper crustal values taken from Taylor and McLennan (1985); Pt is assumed.
MS/ICP-OES/1NAA averaged.

	Method	H-chond.[a]	Mode[b]	Brunflo meteorite samples			Host rock samples																
Distance (mm):				BR3b 0	BR4 0	mean 0	BR10.1 1	BR10.2 4	BR10.3 8	BR10.4 14	BR5 20	BR11 20	BR12 43	BR6 48	BR13 87	BR7 95	BR8 135	BR14 139	BR9 247	BR15 290	average 14–43	average 48–290	BR1
Li	1	1.7		10	4	7	31	10	9	8	10	7	6	11	4	10	12	5	8	5	8	8	11
Be	1	0.04		0.6	0.3	0.4	1.7	0.5	0.3	0.3	0.3	0.1	< 0.1	0.2	< 0.1	0.4	0.4	< 0.1	0.2	< 0.1	0.2	0.3	0.33
Na	2	5700	41	93	60	77	300	309	320	310	n.a.	347	264	n.a.	206	263	362	235	193	230	307	248	210
Mg	4	142 000	2660	1302	505	904	5995	4510	4188	4490	4961	4200	4542	5752	3829	5910	6359	3645	4903	3600	4548	4857	3700
Al	3	10 100	10 000	n.a.	n.a.	–	n.a.	13000	12200	9700	n.a.	14600	20900	n.a.	15800	n.a.	24700	n.a.	15 600	n.a.	15067	18700	15200
K	5	830	6208	6409	5920	6165	9270	5615	6115	4505	n.a.	5835	8740	n.a.	7735	7940	11150	7670	6025	7060	6360	7930	6900
Ca%	2	1.2	23.0	14.6	n.a.	14.6	n.a.	35.0	38.2	33.9	n.a.	34.8	34.0	n.a.	33.2	32.1	29.6	31.5	34.8	33.2	34.2	32.4	34.0
Sc	2	7.6		5.6	3.4	4.5	14.0	9.0	7.6	4.6	n.a.	4.4	5.5	n.a.	4.7	5.1	5.9	5.1	4.3	5.0	4.8	5.0	4.7
Ti	1	620	1572	462	595	528	1522	591	572	563	638	653	671	690	528	788	1234	620	617	647	631	732	824
V	4	61	634	473	464	469	923	173	162	105	131	29	26	123	27	51	36	58	45	21	73	52	20
Cr	2	3400	2791	4360	3190	3775	2440	103	50	33	22	34	29	22	18	26	29	19	17	22	29	22	25
Mn	3	2260	896	n.a.	n.a.	–	n.a.	3150	3050	3000	n.a.	2490	2370	n.a.	2640	n.a.	2244	n.a.	2179	n.a.	2620	2354	2227
Fe%	6	27.60	0.94	0.60	0.49	0.55	0.92	0.57	0.56	0.55	0.81	0.87	1.29	1.06	1.24	1.60	1.51	1.23	1.56	0.9	1.34	1.33	
Co	2	834	7585	3954	5820	4887	48	3.3	3.1	2.9	n.a.	9.7	6.1	n.a.	5.4	5.9	6.8	5.2	5.0	5.1	6.2	5.6	6.9
Ni	1	16 850	7309	2863	5172	4018	106	35	31	38	43	31	35	38	26	39	49	30	34	29	36	35	29
Cu	1	90.0	1231	105	339	222	8.3	0.0	8.0	3.2	18.1	0.0	3.7	5.8	1.7	8.7	16.5	0.0	6.2	0.0	6	5.5	5.8
Zn	1	51	26	84	107	96	65	14	11	15	20	14	12	18	10	15	21	13	14	14	15	15	12
Ga	2(3)	5.2		(4.2)	(5.9)	5.1	n.a	< 7.8	4.	< 19	n.a.	6.5	< 0.1	n.a.	< 21	< 16	< 17	< 36	< 29	< 36			4.1
Ge	1	11.4		4.2	5.5	4.9	4.6	2.5	4.6	1.2	0.6	0.2	< 0.1	1.5	< 0.1	2.1	3.0	0.5	3.6	0.6	0.7	1.9	1.4
As	2(1)	2.0	19094	10755	16400	13578	(78.4)	0.61	0.76	1.7		9.0	0.8	13.0	1.4	1.0	1.0	2.1	1.2	1.2	3.8	3.0	0.7
Se	2	7.0		36.0	n.a.	36.0	n.a.	< 1	< 1	< 1	n.a.	< 1.9	< 1	n.a.	< 1	< 1	< 1.1	0.8	< 1.5	< 1			*0.05*
Rb	5	3		18	17	18	46	26	26	22	29	29	38	36	31	37	57	36	30	35	29	37	31
Sr	5	9.5	3566	7890	n.a.	7890	n.a.	322	300	239	276	248	209	226	207	222	201	223	239	208	243	218	197
Y	1	2.2		13	8	10	11	9	9	9	9	8	9	9	5	9	11	9	9	9	9	9	12
Zr	1	9.5		4	7	5	38	17	19	18	23	30	26	25	21	30	41	26	21	25	24	27	28

Nb	1	0.4		1.1	0.9	1.0	2.1	1.5	2.1	2.0	2.1	2.0	2.1	2.2	1.7	2.4	3.7	1.9	1.6	2.0	2.0	2.2	2.2
Mo	1(7)	1.7		(2832)	(1368)	2100	9.2	< 0.1	0.2	0.1	7.4	87.0	0.1	4.2	0.0	0.3	0.0	0.0	0.1	0.0	24	0.7	0.4
Pd	1	0.91		4.2	1.4	2.8	< 0.1	< 0.1	< 0.1	< 0.1	< 0.1	< 0.1	< 0.1	< 0.1	< 0.1	< 0.1	< 0.1	< 0.1	< 0.1	< 0.1	< 0.1			*0.0005*
Ag	1	0.08		6.7	2.7	4.7	0.60	< 0.1	< 0.1	< 0.1	< 0.1	< 0.1	< 0.1	< 0.1	< 0.1	< 0.1	< 0.1	< 0.1	< 0.1	< 0.1	< 0.1			0.7
Cd	1	0.04		11.3	4.5	7.9	< 0.1	< 0.1	< 0.1	< 0.1	< 0.1	< 0.1	< 0.1	< 0.1	< 0.1	< 0.1	< 0.1	< 0.1	< 0.1	< 0.1	< 0.1			0.04
Sn	1	0.60		1.0	0.4	0.7	0.4	< 0.01	0.4	< 0.01	0.4	0.5	2.1	0.6	1.9	1.1	3.5	0.5	0.3	0.3	1.0	1.2	0.3
Sb	2(5)	0.09		(30)	(31)	30.5	2.2	0.4	0.5	< 0.2	n.a.	0.9	0.7	n.a.	0.8	0.6	1.2	1.1	0.8	0.9	0.8	0.9	0.7
Cs	5(1)	0.09		(1.5)	(2.0)	1.8	2.9	1.2	1.4	1.2	1.5	1.6	2.1	1.8	1.8	2.1	2.9	2.4	1.7	2.0	1.6	2.1	2.1
Ba	5(2)	3.5	138 000	(301000)	n.a.	30100	n.a.	63	69	75	156	80	56	100	75	94	136	83	71	102	92	94	88
La	5	0.30		3.4	2.3	2.8	4.0	5.3	6.4	7.3	6.0	9.7	8.5	5.4	8.2	8.8	8.6	8.8	8.5	9.0	7.9	8.2	11.0
Ce	5	0.84		14.7	7.7	11.2	12.0	16.3	20.5	19.4	16.7	22.2	19.6	13.4	19.0	20.5	24.1	24.9	19.1	22.8	19.5	20.8	24.0
Nd	2	0.58		n.a.	n.a.	–	n.a.	20.1	14.3	10.2	n.a.	14.6	11.6	n.a.	12.7	13.3	11.4	15.1	7.6	11.0	12.1	11.9	13.3
Sm	2	0.21		3.8	n.a.	3.8	n.a.	1.9	2.1	1.7	n.a.	2.2	2.1	2.3	1.8	2.0	2.4	1.7	1.8	1.9	2.0	2.0	2.3
Eu	2	0.07		0.72	n.a.	0.7	n.a.	0.4	0.4	0.4	n.a.	0.6	0.6	n.a.	0.5	0.5	0.6	0.5	0.5	0.5	0.5	0.5	0.5
Tb	2	0.05		< 0.74	n.a.	< 0.74	0.3	0.3	0.3	0.3	n.a.	0.4	0.4	n.a.	0.3	0.3	0.4	0.4	0.3	0.3	0.4	0.3	0.4
Yb	2	0.17		0.8	n.a.	0.8	n.a.	1.0	0.8	0.9	n.a.	1.1	1.1	n.a.	1.0	1.1	1.2	1.1	1.0	1.0	1.0	1.1	0.9
Lu	2	0.03		< 0.32	n.a.	< 0.32	n.a.	0.1	0.2	0.1	n.a.	0.2	0.2	n.a.	0.1	0.2	0.2	0.2	0.1	0.1	0.2	0.1	0.1
Hf	5	0.25		0.6	0.4	0.5	0.9	0.6	0.6	0.6	0.7	1.2	1.3	0.7	0.9	1.1	1.4	1.0	0.6	0.9	1.0	0.9	1.1
Ta	2	0.02		1.7	n.a.	1.7	n.a.	< 0.25	0.3	0.2	n.a.	0.2	0.4	n.a.	0.2	0.3	0.3	0.2	< 0.35	0.2	0.3	0.2	0.2
W	1	0.14		0.5	1.3	0.9	0.9	< 0.1	0.6	< 0.1	0.6	0.5	1.1	0.3	0.8	0.5	1.2	1.4	1.0	1.2	0.7	0.9	1.0
Re	2	0.08		1.9	n.a.	1.9	n.a.	n.a.	n.a.	n.a.	n.a.	n.a.	n.a.	n.a.	n.a.	n.a.	n.a.	n.a.	n.a.	n.a.			*0.0005*
Pt	1	1.50		0.9	1.0	1.0	n.a.	n.a.	n.a.	n.a.	n.a.	n.a.	n.a.	n.a.	n.a.	n.a.	n.a.	n.a.	n.a.	n.a.			*0.0005*
Ir	2	0.77		0.64	n.a.	0.64	n.a.	n.a.	n.a.	n.a.	n.a.	n.a.	n.a.	n.a.	n.a.	n.a.	n.a.	n.a.	n.a.	n.a.			*0.00002*
Au	2	0.23		0.2	1.2	0.71	2.5	0.006	0.005	0.004	n.a.	< 0.01	< 0.01	n.a.	0.004	0.040	< 0.08	< 0.01	< 0.01	< 0.01	0.004	0.022	0.0025
Tl	1	0.001		4.6	2.9	3.8	0.3	< 0.1	< 0.1	0.2	0.2	0.9	0.2	0.2	0.1	0.2	0.1	0.3	< 0.1	1.3	0.4	0.4	0.04
Pb	1	0.24		151	113	132	62	0.6	0.9	1.1	1.7	4.7	2.2	1.2	2.6	1.3	1.3	4.7	1.3	6.5	2.4	2.7	2.6
Bi	1	0.003		63	34	48	0.4	< 0.1	0.1	< 0.1	0.2	1.8	< 0.1	0.2	< 0.1	< 0.1	< 0.1	0.1	< 0.1	< 0.1			0.020
Th	2	0.04		< 1.2	n.a.	< 1.2	n.a.	2.7	3.4	3.2	n.a.	11.7	5.4	n.a.	19.7	5.6	5.1	46	4.9	10.6	6.8	15.3	2.6
U	2(1)	0.01		39	(11)	25	240	4.9	1.6	1.0	(1.2)	3.7	1.0	(2.1)	6.4	1.3	0.7	21	1.3	3.3	1.7	5.2	0.44
Ni/Co		20.2	1.0	0.7	0.9	0.8	2.2	10.6	10.1	12.9		3.2	5.7		4.8	6.5	7.1	5.8	6.8	5.6	5.9	6.3	4.2

[a] average H chondrite values, from Mason (1971).
[b] concentrations obtained from mode and mineral compositions, see text.

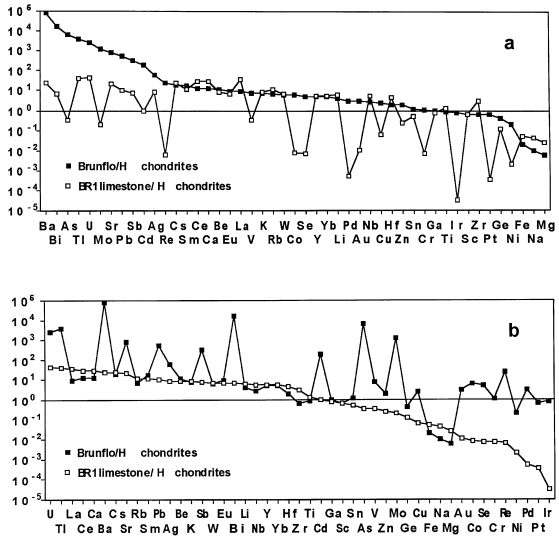

Fig. 4. H chondrite-normalized plots for the Brunflo chondrite and limestone sample BR1 from the same stratigraphic level as Brunflo. In diagram a elements are arranged in order of decreasing enrichment or increasing depletion in Brunflo. In diagram b, elements are arranged in order of decreasing ratios of concentrations in limestone to H chondrite, illustrating the inital concentration gradients between the freshly fallen meteorite and the sediment. Normalization values are given in Table 5.

6.80:0.1, Al = 1.00:1.01, Si = 2.96:16.95, S = 4.60:2.00, Mn = 0.09:0.23.

The most strongly depleted elements are Na (0.01), Fe (0.02), Mg (0.1), Si (0.17), Ni (0.2) and Mn (0.3). The meteoritic nature of Brunflo is confirmed by concentrations of Ir, Pt and Au close to average chondritic values. Considering the pervasive alteration, our chemical data cannot be used to verify the classification as H chondrite based on chromite composition and chondrule types (Thorslund et al., 1984).

5.6. Host rock geochemistry

Concentrations for up to 46 elements in cores from the limestone surrounding the Brunflo chondrite are presented in Table 5 and Figs. 5–7. Comparison of all analytical results for reference sample BR1 (Table 4) shows that the ICP-MS and INAA methods which were used to produce most of the data for the limestone cores, yield results consistent with ICP-OES, XRF, GFAA (graphite-furnace atomic absorption) and INAA as determined by other laboratories. The methods used in order to calculate the average of each element are given in Table 5.

Average values for the cores drilled 14–45 mm (4 samples) and 48–290 mm (7 samples) from the meteorite are also given. Uncertainties in the element concentration trends arise because the host rock is heterogeneous at the scale of the small core samples. This is evident in the profiles of immobile elements such as Sc, Ti and Zr (Fig. 6h). Only large and systematic deviations of element concentrations from the average limestone values can therefore be ascertained. A comparison of the average values for the limestone near the meteorite (14–45 mm distance) with sample BR1 is presented in Fig. 5. From these average values, enrichments of As, U, V, Th and Na and depletions of Fe and Li can be deduced. The reason for increased Th concentrations near the meteorite and in the 48–290 mm zone is unclear and may possibly be due to higher levels in the limestone hosting Brunflo compared with the BR1 value. These increased Th levels are correlated with U of probable detrital origin from sample BR10.3 outwards.

For better recognition of element mobilization trends, the analytical data were normalized to the inferred initial concentrations. ''Best values'' of BR1 (Table 4) were used to normalize limestone core samples and the average H chondrite values of Mason (1971) for the meteorite. Sample BR10.1, composed of limestone and meteorite, was normalized to a mixture of 0.565 chondrite + 0.435 BR1 limestone based on Cr content. Normalized element concentration profiles for a range of elements with different behavior are illustrated in Fig. 6. Three basic types of concentration profiles can be distinguished.

(I) Depleted elements: Examples are Fe, Mn, Na, Mg, Ni (Fig. 6a,b). Most of these elements are

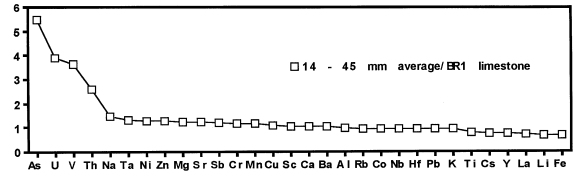

Fig. 5. Ratios of averaged element concentrations in limestone samples 14–45 mm from the chondrite to limestone reference sample BR1, arranged in decreasing order.

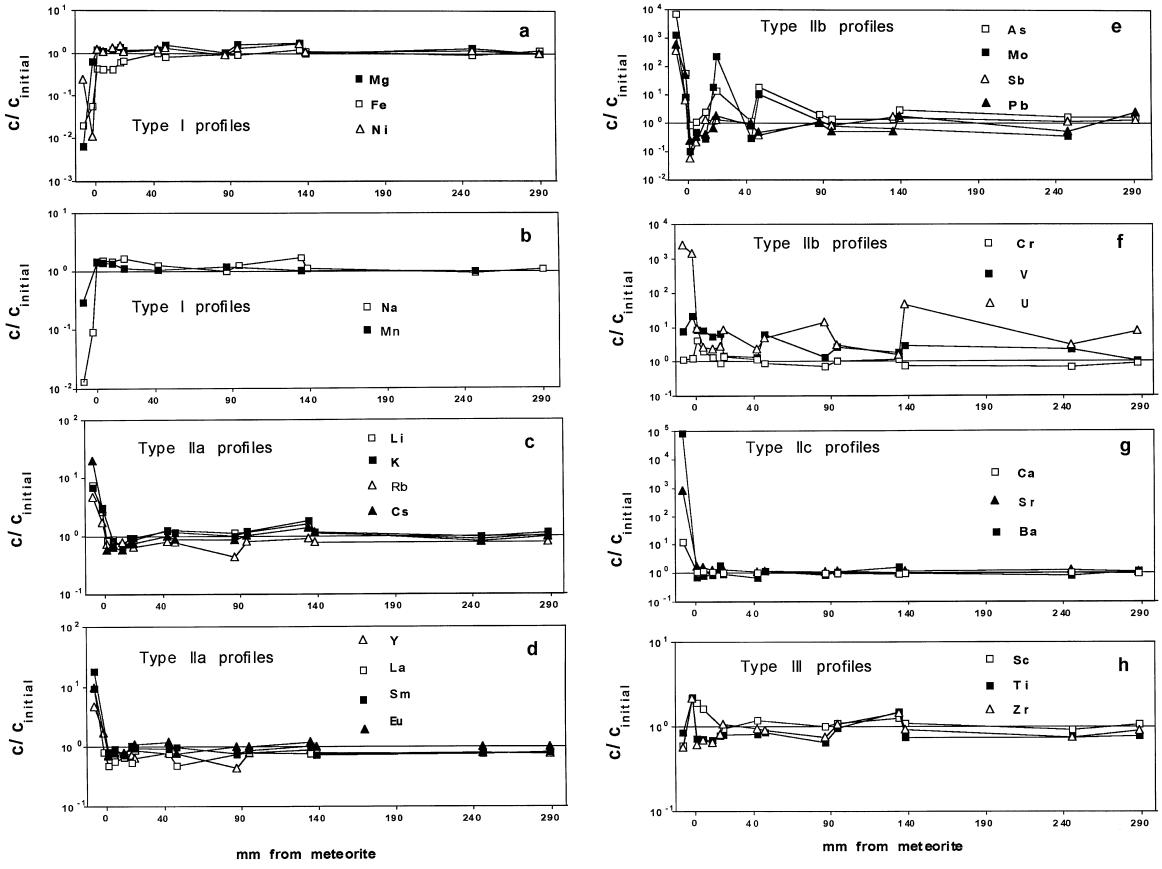

Fig. 6. Background-normalized element profiles (see text) of the Brunflo chondrite and adjoining limestone.

depleted in the meteorite only, but the depletion of Fe extends into the limestone. Some of the Na and Mn lost from the meteorite seem to have accumulated in the surrounding limestone.

(II) Enriched elements: Elements insensitive to redox conditions like alkalis and REE (IIa profiles, Fig. 6c,d) were probably enriched due to incorporation into newly formed silicates. These elements are slightly depleted near the meteorite. Redox sensitive elements like V, As, Mo, U (type IIb profiles, Fig. 6e,f) show very strong enrichment in the meteorite and, in some cases, close to the meteorite; As and Mo appear to be depleted in the contact zone. Alkaline earths (type IIc profiles, Fig. 6g) show no evidence of mobility in the limestone with the exception of a slight enrichment of Ca near the meteorite (Table 5).

(III) Elements showing little evidence of mobility besides a concentration spike in the contact zone sample (Fig. 6h).

The low bulk Ni/Co ratio of 0.82 in the meteorite, compared to a chondritic value of 20.2, demonstrates that significant and large-scale redistribution of Ni and Co have taken place (Fig. 7a,b). Nickel is depleted in the meteorite and in contact sample BR10.1 (type I profile); some of the lost Ni is taken up in the limestone near the meteorite. Cobalt is enriched in the meteorite, but depleted in the contact sample and in the immediately surrounding limestone up to a distance of about 15 mm (Fig. 7a). A comparison of present and calculated initial Ni/Co ratios (Fig. 7b) clearly shows that Co has been added to the meteorite and Ni has been lost into surrounding limestone.

Both V and Cr have type IIb profiles (Fig. 6f) with a much lower enrichment factor for Cr due to its high initial concentration in the meteorite. The distribution of V and Cr in the limestone at the meteorite contact was further investigated by microprobe analysis in six profiles of 4 to 5 mm length perpendicular to the contact. Representative concentration profiles for V and Cr are presented in Fig. 8a. Absolute concentrations of Cr and V generally decrease away from the meteorite, from maximum values around 0.3% to below background (0.02%) over a distance of about 4 mm. The Cr/V ratio (Fig. 8b) decreases slightly away from the meteorite. The average ratio of 0.84 is similar to the value of 0.94 determined by microprobe analysis of the phyllosilicate within the meteorite (Nyström and Wickman, 1991). Considering the fact that Cr/V ratios typically increase in profiles from lower to higher redox potential in low-temperature redox fronts (Breit and Goldhaber, 1989), the rise in Cr/V towards the meteorite is probably caused by partial supply of Cr from the meteorite while V was predominantly supplied from an external source.

5.7. Sulfur isotopes

The sulfur isotope composition of barite from the meteorite was determined in order to test the assumption that the sulfur in the altered meteorite (3.3 wt.% as barite) was derived from the oxidation of sulfide sulfur in meteoritic troilite (2.0–3.0% S in H chondrites). The results show that barite sulfur is too heavy ($\delta^{34}S = +35‰$ relative to CDT) to be derived from chondritic troilite ($\delta^{34}S - 0.02 \pm 0.06‰$, Gao and Thiemens, 1993). Ordovician seawater with $\delta^{34}S$ values of $+30$ to $+35‰$ (Claypool et al., 1980) is, however, a likely source. Thus, it must be assumed that almost all the meteoritic S was lost prior to precipitation of marine sulfate as barite.

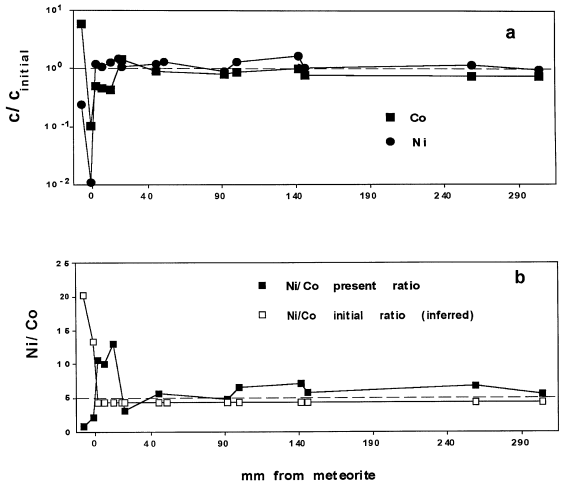

Fig. 7. (a) Background-normalized profiles for Ni and Co and (b) Ni/Co ratio profiles as measured compared with inferred primary ratios.

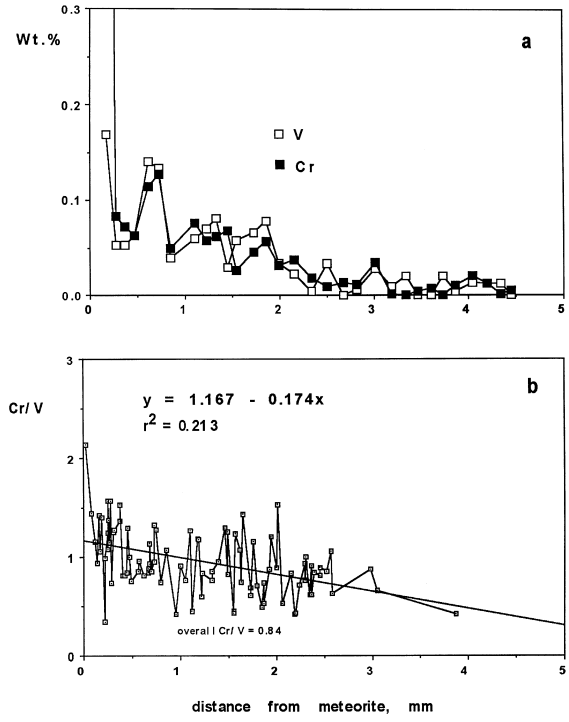

Fig. 8. Variations in (a) V and Cr contents in a representative profile, and (b) the average Cr/V ratio in six profiles (electron microprobe data), in limestone at the meteorite contact. High Cr value 0.2 mm from the contact in (a) is due to the presence of chromite grains derived from the partially disintegrated meteorite.

6. Discussion

6.1. Geochemistry and mineralogy of meteorite alteration

Because the primary meteoritic minerals are replaced by a mineral assemblage low in Si, Mg and

Fe, but dominated by calcite, barite and V–Cr-bearing illite, dissolution of silicates, nickel–iron and troilite may be summarized with the following overall reactions:

olivine: $(Mg_{0.8}Fe_{0.2})_2SiO_4 + 4H_2O \rightarrow 1.6Mg^{2+} + 0.4Fe^{2+} + H_4SiO_4 + 4OH^-$

pyroxene: $(Mg_{0.8}Fe_{0.2})SiO_3 + 3H_2O \rightarrow 0.8Mg^{2+} + 0.2Fe^{2+} + H_4SiO_4 + 2OH^-$

nickel–iron: $Fe + 2H_2O \rightarrow Fe^{2+} + 2OH^- + H_2$ (anaerobic Ni and Co behave as Fe)

$4Fe + 3O_2 + 2H_2O \rightarrow 4FeOOH$ (aerobic, Ni and Co behavior uncertain)

troilite: $FeS + 2H_2O \rightarrow Fe^{2+} + H_2S + 2OH^-$ (anaerobic)

$4FeS + 9O_2 + 6H_2O \rightarrow 4FeOOH + 4SO_4^{2-} + 8H^+$ (aerobic)

Silicate hydrolysis caused a rise of pH in the porewater within the meteorite and precipitation of calcite. The resulting Ca concentration difference in the porewater caused inward diffusion of Ca and explains the calcitization of the silicate-rich meteorite according to the bulk reaction:

$$(Mg_{0.8}Fe_{0.2})_2SiO_4 + 4Ca^{2+} + 4HCO_3^- \rightarrow 4CaCO_3 + 1.6Mg^{2+} + 0.4Fe^{2+} + H_4SiO_4$$

Most of the Mg, Fe and Si were subsequently lost from the meteorite.

Hydrolysis and formation of new silicate, precipitation of barite and calcite and redox reactions are responsible for the intense redistribution of elements in the meteorite and surrounding limestone. The depletion in Si, Na, Fe, Mg, Ni and Mn, and enrichment in Ba, As, U, Mo, V, Co, Cu and Zn are confirmed by mineralogical evidence. The enrichment in redox-sensitive transition group elements such as As, U, Mo and V can be explained by reduction of oxidized mobile species to reduced forms of low solubility. The enrichment in a number of other elements, e.g., Ba, Sr, Co, Cs and REE, cannot be explained by redox processes and most likely is due to coprecipitation during precipitation of barite, silicate and other minerals. Even though barite has been described as an alteration product in weathered chondrites (Bischoff and Geiger, 1995), the mechanism of barite formation may be different in Brunflo since the barite here is a relatively late mineral according to its S isotope composition.

6.2. Geochemistry of alteration in the limestone around the meteorite

The profiles of 14 limestone samples at distances varying between 0 and 290 mm from the contact with the meteorite show clear evidence of element redistribution up to at least 20 mm from the contact in the case of Fe and V. For most other elements, there is evidence of significant redistribution only close to the meteorite. All observed element variations are within zones I and II. It must be assumed that Fe was retained in the limestone in a reduced form where the element is not depleted but a color change is observed.

The three main types of element profiles described in Section 5.6. and illustrated in Fig. 6 may be explained by the following styles of element behavior:

Type I profiles characterize elements that were mobilized during the alteration of the meteorite due to dissolution of meteoritic phases. These elements partially reaccumulated in surrounding limestone.

Type II profiles developed in the case of mobile elements that precipitated in and near the meteorite due to neoformation of minerals such as silicates (type IIa), reduced assemblages (type IIb), and barite and calcite (type IIc). Most of these elements must have been transported over considerable distance because generally no depletion zone near the meteorite is evident. Precipitation of elements due to reduction occurred at a distance of up to 20 mm from the meteorite.

Type III profiles result from the strong chemical gradient at the contact leading to the enrichment of elements that otherwise are considered as immobile: Sc, Ti, Zr and Hf.

Strongly contrasting behavior of Ni and Co under reducing conditions is unusual and different from that in reduction spots (Hofmann, 1990, 1991) where both elements are enriched to about the same degree. However, preferential mobilization of Ni appears to be common during alteration of meteorites under oxidizing conditions (Buddhue, 1957; White et al.,

1967; Golden et al., 1995). Oxidizing conditions within the meteorite should generate abundant Fe-hydroxide which is not found in Brunflo. The temporary presence of Fe-hydroxides during early stages of alteration could be a possible explanation for the observed Ni-Co fractionation.

The redox mass balance of Brunflo can be calculated from the estimated meteorite mass (Table 3), typical H chondrite bulk compositions and the Fe concentration profile in the host rock (Table 5). The amount of Fe lost from the limestone adjacent to the meteorite was calculated with a model assuming spherical shells of 1 cm thickness from 0 to 15 cm distance from the meteorite and using the average measured Fe concentration for each distance. The results, given in Table 6, demonstrate that the reductive dissolution of hematite around Brunflo was possible with only a fraction (2–60%, best estimate 11%) of the total available reduction capacity of nickel-iron and troilite.

Table 6
Redox mass balance for Brunflo

Reduction capacity of meteorite estimated from assumed primary composition			
		Average	Possible range
Meteorite volume (Table 3)	cm^3	357	200–700
Meteorite density (Mason, 1971)	g/cm^3	3.7	3.4–3.9
Meteorite weight (Table 3)	g	1303	680–2730
Metallic Fe (Mason, 1971)	wt%	16.5	14.0–19.0
S as FeS (Mason, 1971)	wt%	2.0	0.9–2.6
Metallic Fe	g	215	95–519
Sulfide S	g	26	6–71
Metallic Fe	moles	3.85	1.70–9.29
S as FeS	moles	0.81	0.19–2.21
Reduction capacity of Fe	eq	7.7	3.4–18.6
Reduction capacity of sulfide S	eq	6.5	1.5–17.7
Total reduction capacity	eq	14.2	4.9–36.3
Reduction capacity of meteorite estimated from Fe concentration profile			
		Best estimate	Possible range
Fe dissolved around meteorite	g	85	37–160
Fe dissolved	moles	1.52	0.6–2.9
Reduction capacity needed	eq	1.52	0.6–2.9

The Fe concentration shows a peak at the meteorite–limestone contact (sample BR10.1; Table 5). It is due to the presence of microcrystalline hematite and also corresponds to the site of highest U concentration. Similar hematite enrichment is common immediately adjacent to U-rich minerals (Heinrich, 1958) and probably results from Fe oxidation induced by oxidizing species produced by radiolysis of porewater (Vovk, 1987).

A comparison between patterns of element mobility in reduction spots (Hofmann, 1990, 1991) and in Brunflo suggests similar processes of reductive accumulation/mobilization for many elements (V, Cr, Fe, Co, Cu, Zn, As, Se, Ag, Cd, Sb, PGE, Au, Pb, Bi and U). The behavior of Ni, Mo and Re is different. In reduction spots the hematite dissolution front is generally very sharp while in Brunflo it is diffuse.

6.3. An alteration scenario for the Brunflo chondrite

Reactive reductants present in the freshly fallen Brunflo chondrite were nickel-iron (kamacite and taenite), troilite and ferrous silicates. Based on mass balance calculations (Table 6), the amounts of metallic Fe and FeS appear to have been sufficient to produce the observed reductive alterations, mainly the reductive dissolution of hematite responsible for the visible zonation around the meteorite.

Considering the low sedimentation rate of 0.2–0.3 cm/1000 years, the meteorite must have interacted with oxygenated porewaters for several 100 000 years after the fall. Under continental conditions, chondritic meteorites are completely weathered within a few thousand years (Boeckl, 1972; Bischoff and Geiger, 1995). It is thus likely that Fe and FeS in the meteorite were oxidized to an assemblage of Fe-hydroxides (possibly including akaganéite, Buchwald and Clarke, 1989) while the meteorite was buried under only a few millimeters to a few centimeters of sediment. Initial alteration under oxygenated conditions might explain the contrasting behavior of Ni and Co that resembles the behavior during continental weathering of iron meteorites (Buddhue, 1957;

White et al., 1967; Golden et al., 1995). However, evidence from the more oxidized Österplana meteorites in red limestones with nearly chondritic Ni/Co (discussed under Section 6.4) indicates that Ni/Co fractionation more likely occurred under reducing conditions. Troilitic S was lost during early burial. Chromite was partially corroded leading to the development of a Cr halo about 10 mm wide around the meteorite. Accumulation of trace elements may have occurred during this stage due to adsorption to Fe hydroxides and/or redox processes. Accumulation of U during oxidative terrestrial weathering of meteorites has been described by Delisle et al. (1989) and Hofmann (1992b).

During deeper burial, porewaters became less oxidizing although they were still in equilibrium with hematite in the bulk rock. At this stage, only a small part of the silicate-bound ferrous iron may have remained as reductant in the meteorite. Reduction by ferrous iron cannot explain the halo of reduced Fe around the meteorite. The reduction processes during this stage must have been supported by still unoxidized meteoritic minerals or, more likely, externally derived mobile reductants, e.g., hydrocarbons or H_2 possibly derived from the underlying alum shale. Catalysts present in the meteorite (e.g., platinum group elements) may have promoted redox reactions. This second stage of alteration may well have occurred during Caledonian nappe tectonism. Evidence of Caledonian Ba mobility in the alum shale has been provided by Leventhal (1991). A reduction process with an externally derived reductant is similar to models proposed for the formation of reduction spots in red beds (Hofmann, 1990, 1991, 1992a). Among the many similarities between the two types of reduction phenomena is the presence of small amounts of sulfide produced in situ by sulfate reduction.

6.4. Comparison with other fossil meteorites

Element concentration data for fossil stony meteorites and limestone host rocks from a stratigraphically similar position at Österplana, southern Sweden (Schmitz et al., 1996, 1997) are compared with our Brunflo data in Table 7. The main alteration products in the Österplana meteorites are calcite and in part barite as in the case of Brunflo. The behavior of Ni and Co is different. Both elements are lost almost entirely at Österplana, with Ni/Co values remaining close to chondritic ratio. The only exception is a single meteorite from a gray bed that is enriched in Co like Brunflo, indicating that Ni/Co fractionation is favored by reducing conditions. Another difference is the lack of Mo enrichment at Österplana. The Österplana host rock data are very similar to the values for sample BR1, indicating that variations in host rock geochemistry cannot account for the differences observed in the meteorites, but rather the redox conditions during diagenesis and/or the thermal history. Differences in element behavior at Brunflo and Österplana suggest that element mobilities were late diagenetic. Early diagenetic processes were probably very similar at both sites.

Table 7
Comparison of analyses for Brunflo and Österplana fossil meteorites
Österplana meteorite data are from Schmitz et al. (1997), Table 1. Fe, Ca and Ba originally reported low by a factor of 10 (B. Schmitz, personal communication, 1997).
Österplana limestone data are from Schmitz et al. (1996), Table 1, red limestone only.

Fossil meteorites	Brunflo	Österplana ($n = 8$)	
		x	s
Ca%	14.6	27.7	10.2
Cr ppm	3775	4147	1926
Fe%	0.55	3.61	2.00
Co ppm	4887	16[a]	5.9[a]
Ni ppm	4018	302[a]	161[a]
As ppm	13600	296[b]	
Mo ppm	2100	< 2[b]	
Ba%	30.1	9.88	12.4
Ir ppb	640	372	340
Au ppb	710	190	217
Ni/Co	0.82	19.2[a]	13.3[a]
Host limestone	**Brunflo (BR1)**	**Österplana ($n = 29$)**	
		x	s
Sc ppm	4.7	4.6	2.8
Fe%	1.33	1.61	1.27
Ni ppm	29	24	20.0
Co ppm	6.9	7.4	5.8
Cr ppm	25	21.2	17.8
Sb ppm	0.7	0.8	0.6
Th ppm	2.6	4.9	4.0

[a]One sample in gray limestone with Ni 969 ppm, Co 2100 ppm (Ni/Co = 0.46) excluded.
[b]Single data.

A small fossil meteorite from K/T boundary sediments in the North Pacific Ocean (Kyte, 1998) was buried under a maximum of 55 m of sediments at temperatures not exceeding 5°C (Kyte, 1998). Even under these conditions, significant chemical changes including enrichments of Au and As were detected (Kyte, 1998).

6.5. Comparison with Co–Ni–Bi–Ag–U-mineralizations

The enrichment in Co, Ni, As, U, Bi and Ag (with Co > Ni) and the presence of Co–Ni-arsenides in Brunflo constitute a strong similarity with some economic and non-economic mineralizations. These include hydrothermal veins of the five-elements suite (Ni–Co–As–Ag–Bi) like Cobalt and Bear Lake in Canada and the Erzgebirge, Germany (Kissin, 1993), unconformity-related uranium deposits in Canada and Australia (Dahlkamp, 1978; Wilde et al., 1989) and reduction spots in red bed sediments (Hofmann, 1990, 1991). Besides showing the above-mentioned pattern of enrichment, these occurrences typically contain native elements (Ag, Bi, Sb, As) and sulfides, especially pyrite, are absent or occur in low amounts. While element precipitation likely is related to reduction of As, U, Ag etc., the reason for the scarcity of sulfides (especially of Fe) and details of the precipitation mechanisms remains unclear (Kissin, 1993).

7. Conclusions

The inferred initial elemental concentrations in Brunflo and surrounding limestone have been strongly disturbed by alteration processes. Based on the geological situation, we conclude that the first stage of alteration occurred under oxidizing conditions and resulted in the oxidation and loss of nickel–iron and troilite.

During a second stage, under conditions of deeper burial, reduction processes occurred within and around the meteorite that cannot have been supported by the reduction capacity left after the first stage of alteration. A catalytic action by trace elements in the meteorite on inert reductants derived, for example, from underlying alum shale, may be inferred. Redox- and pH-driven reactions and coprecipitation were the main processes involved in element redistribution.

The alteration of Brunflo demonstrates that concentrations of most elements in chondritic meteorites can change drastically during terrestrial alteration. Present proportions between Fe, Ni and Co may be grossly misleading. The high Ir, Pt and Au concentrations in proportions similar to those in H chondrites constitutes a third, independent line of evidence for a meteoritic origin, besides the well-preserved chondritic structure and presence of relict chromite.

Two features of Brunflo remain difficult to understand: (a) Although barite precipitation might be explained by troilite oxidation in terms of mass balance, this origin is inconsistent with the heavy sulfur isotope signature of the barite, which indicates initial mobilization of meteoritic S and later accumulation of marine sulfate S due to barite precipitation, for unknown reasons; (b) The contrasting behavior of Ni and Co under oxidizing conditions and in the presence of reduced As. Later reduction may be explained by an externally derived reductant.

The behavior of many elements in Brunflo (e.g., V, U and Mo) is similar to that in certain economic and non-economic mineral deposits whose formation is related to redox boundaries, for example roll front U and tabular V–U deposits in sandstones, reduction spots in red beds, unconformity-related U deposits and vein-type Ni–Co–As–Ag–Bi–deposits. The reason for these similarities remains unclear at present.

Acknowledgements

This paper is part of a wider project on redox geochemistry for which support by Nagra (Swiss national cooperative for the disposal of radioactive waste) is gratefully acknowledged. Lars Karis (Geological Survey of Sweden) kindly supplied the reference sample of Brunflo limestone. We thank R. Mäder and H. Oschidari (Bern University) for sample preparation and analytical support. We thank H.Y. McSween and P. Bland for constructive reviews. The electron microprobe at Bern University, used during this study, is supported by the Swiss National Science foundation (grant 21-26579.89).

References

Bergström, S.M., 1980. Conodonts as palaeotemperature tools in Ordovician rocks of the Caledonides and adjacent areas of Scandinavia and the British Isles. Geol. För. Stockholm Förh. 102, 377–392.

Bergström, J., Gee, D.G., 1985. The Cambrian in Scandinavia. In: Gee, D.G., Sturt, B.A. (Eds.), The Caledonide Orogen — Scandinavia and Related Areas. Wiley, pp. 247–261.

Bischoff, A., Geiger, T., 1995. Meteorites from the Sahara: find locations, shock classification, degree of weathering and pairing. Meteoritics 30, 113–122.

Boeckl, R.S., 1972. Terrestrial age of nineteen stony meteorites derived from their radiocarbon content. Nature 236, 25–26.

Breit, G.N., Goldhaber, M., 1989. Hematite-enriched sandstones and chromium-rich clays — clues to the origin of vanadium-uranium deposits in the Morrison-Formation, southwestern Colorado and southeastern Utah. IAEA-TECDOC 500, 201–225.

Bruton, D.L., Lindström, M., Owen, A.W., 1985. The Ordovician of Scandinavia. In: Gee, D.G., Sturt, B.A. (Eds.), The Caledonide Orogen — Scandinavia and Related Areas. Wiley, pp. 273–282.

Buchwald, V.F., Clarke, R.S. Jr., 1989. Corrosion of Fe–Ni alloys by Cl-containing akaganéite (β-FeOOH): The Antarctic meteorite case. Am. Mineral. 74, 656–667.

Buddhue, J.D., 1957. The oxidation and weathering of meteorites. Univ. of New Mexico Press, Albuquerque, p. 161.

Bunch, T.E., Keil, K., Snetsinger, K.G., 1967. Chromite composition in relation to chemistry and texture of ordinary chondrites. Geochim. Cosmochim. Acta 31, 1569–1582.

Claypool, G.E., Holser, W.T., Kaplan, I.R., Sakai, H., Zak, I., 1980. The age curves of sulfur and oxygen isotopes in marine sulfate and their mutual interpretation. Chem. Geol. 28, 199–260.

Dahlkamp, F.J., 1978. Geologic appraisal of the Key Lake U–Ni deposits, northern Saskatchewan. Econ. Geol. 73, 1430–1449.

Delisle, G., Schultz, L., Spettel, B., Weber, H.W., Wlotzka, F., Höfle, H.-Ch., Thierbach, R., Vogt, S., Herpers, U., Bonani, G., Suter, M., Wölfli, W., 1989. Meteorite concentrations and glaciological parameters near the Frontier Mountain Range. North Victoria Land. Geol. Jahrb. E38, 483–513.

Gao, X., Thiemens, M.H., 1993. Variations of the isotopic composition of sulfur in enstatite and ordinary chondrites. Geochim. Cosmochim. Acta 57, 3171–3176.

Golden, D.C., Ming, D.W., Zolensky, M.E., 1995. Chemistry and mineralogy of oxidation products on the surface of the Hoba nickel–iron meteorite. Meteoritics 30, 1690–1705.

Heinrich, E.W., 1958. Mineralogy and Geology of Radioactive Raw Materials. McGraw-Hill, New York, p. 654.

Hofmann, B.A., 1990. Reduction spheroids from northern Switzerland: Mineralogy, geochemistry and genetic models. Chem. Geol. 81, 55–81.

Hofmann, B.A., 1991. Mineralogy and geochemistry of reduction spheroids in red beds. Mineral. Petrol. 44, 107–124.

Hofmann, B.A., 1992a. Isolated reduction phenomana in red beds: A result of porewater radiolysis? In: Kharaka, Y.K., Maest, A.S. (Eds.), Water–Rock Interaction, Balkema, Rotterdam, pp. 503–506.

Hofmann, B.A., 1992b. Uranium accumulation during weathering of Cañon Diablo meteoritic iron. Meteoritics 27, 101–103.

Hofmann, B.A., 1999. Geochemistry of natural redox fronts — a review. Nagra Technical Report 99-05, Nagra (National Cooperative for the disposal of radioactive waste), Wettingen, Switzerland.

Jaanusson, V., 1976. Faunal dynamics in the Middle Ordovician (Viruan) of Baltoscandia. In: Basset, M.G. (Ed.), The Ordovician System: Proceedings of a Palaeontological Association symposium, Birmingham, September 1974. Univ. of Wales Press and National Museum of Wales, Cardiff, pp. 301–236.

Jaanusson, V., 1982. Introduction to the Ordovician of Sweden. Palaeontol. Contrib. Univ. Oslo 279, 1–9.

Kisch, H.J., 1980. Incipient metamorphism of Cambro-Silurian clastic rocks from Jämtland Supergroup, central Scandinavian Caledonides, western Sweden: illite crystallinity and vitrinite reflectance. J. Geol. Soc. London 137, 271–288.

Kisch, H.J., 1991. Illite crystallinity: recommendations on sample preparation, X-ray diffraction settings, and interlaboratory samples. J. Metamorphic Geol. 9, 665–670.

Kissin, S.A., 1993. Five-element (Ni–Co–As–Ag–Bi) veins. In: Sheahan, P.A., Cherry, M.E. (Eds.), Ore Deposit Models, Vol. II. Geoscience Canada reprint series 6, pp. 87–98.

Kyte, F.T., 1998. A meteorite from the Cretaceous/Tertiary boundary. Nature 396, 237–239.

Leventhal, J.S., 1991. Comparison of organic geochemistry and metal enrichment in two black shales: Cambrian Alum Shale of Sweden and Devonian Chattanooga Shale of United States. Mineral. Deposita 26, 104–112.

Lindström, M., Sturkell, E.F.F., 1992. Geology of the Early Palaeozoic Lockne impact structure, Central Sweden. Tectonophysics 216, 169–185.

Lindström, M., Sturkell, E.F.F., Törnberg, R., Ormö, J., 1996. The marine impact crater at Lockne, central Sweden. GFF 118, 193–206, previously Geol. För. Stockholm Förh.

Löfgren, A., 1978. Arenigian and Llanvirnian conodonts from Jämtland, northern Sweden. Fossils Strata 13, 1–129.

Mason, B., 1971. Handbook of elemental abundances in meteorites. Gordon & Breach, New York.

McSween, H.Y. Jr., Bennett, M.E. III, Jarosewich, E., 1991. The Mineralogy of ordinary chondrites and implications for asteroid spectrophotometry. Icarus 90, 107–116.

Miller, W., Alexander, R., Chapman, N., McKinley, I., Smellie, J., 1994. Natural analogue studies in the geological disposal of radioactive waste. Studies in Environmental Science 57. Elsevier, Amsterdam, p. 395.

Nyström, J.O., Wickman, F.E., 1991. The Ordovician chondrite from Brunflo, central Sweden: II. Secondary minerals. Lithos 27, 167–185.

Nyström, J.O., Lindström, M., Wickman, F.E., 1988. Discovery of a second Ordovician meteorite using chromite as a tracer. Nature 336, 572–574.

Puura, V., Suuroja, K., 1992. Middle Ordovician astrobleme at Kärdla, Hiiumas Island, West Estonian Archipelago. Meteoritics 27, 279.

Schmitz, B., Lindström, M., Asaro, F., Tassinari, M., 1996. Geochemistry of meteorite-rich marine limestone strata and fossil meteorites from the lower Ordovician at Kinnekulle, Sweden. Earth Planet. Sci. Lett. 145, 31–48.

Schmitz, B., Peucker-Ehrenbrink, B., Lindström, M., Tassinari, M., 1997. Accretion rates of Meteorites and cosmic dust in the Early Ordovician. Science 278, 88–90.

Taylor, S.R., McLennan, S.M., 1985. The continental crust: its composition and evolution. Blackwell, p. 312.

Therriault, A.M., Lindström, M., 1995. Planar deformation features in quartz grains from the resurge deposit of the Lockne structure, Sweden. Meteoritics 30, 700–703.

Thorslund, P., Wickman, F.E., 1981. Middle Ordovician chondrite in fossiliferous limestone from Brunflo, central Sweden. Nature 289, 285–286.

Thorslund, P., Wickman, F., Nyström, J.O., 1984. The Ordovician chondrite from Brunflo, central Sweden, I. General description and primary minerals. Lithos 17, 87–100.

Vovk, I.F., 1987. Some geochemical and mineralogical peculiarities of deposits of radioactive materials as evidence of radiolysis in nature. In: Côme, B., Chapman, N.A. (Eds.), Natural Analogues in Radioactive Waste Disposal. CEC Radioactive Waste Management Series, EUR 11037, Luxembourg, pp. 113–157.

White, J.S., Henderson, E.P., Mason, B., 1967. Secondary minerals produced by weathering of the Wolf Creek meteorite. Am. Mineral. 52, 1190–1197.

Wilde, A.R., Bloom, M.S., Wall, V.J., 1989. Transport and deposition of gold, uranium, and platinum-group elements in unconformity-related uranium deposits. Econ. Geol. Monograph 30, 637–650.